Influence of Molecular Weight and Regioregularity on the Polymorphic Behavior of Poly(3-decylthiophenes)

S. V. Meille,* V. Romita, and T. Caronna

Dipartimento di Chimica, Politecnico di Milano, Via Mancinelli 7, 20133 Milano, Italia

Andrew J. Lovinger

Bell Laboratories, Lucent Technologies, 600 Mountain Avenue, Murray Hill, New Jersey

M. Catellani and L. Belobrzeckaja

Istituto di Chimica delle Macromolecole INMITER-CNR, Via Bassini 15, 20133 Milano, Italia

Received May 9, 1997; Revised Manuscript Received September 5, 1997[⊗]

ABSTRACT: High molecular mass and high regioregularity favor the more common polymorph (form I) of poly(3-alkylthiophenes) and substantially extend toward high temperatures the existence domain of the 2D mesomorphic phase, which these systems access above 70−80 °C. Morphological observations indicate that in thin films of form I the planar polythiophene main chains lie roughly edge-on parallel to the film surface, while side chains are approximately orthogonal to the substrate. Evidence relative to the second polymorph (form II), easily obtained with low-molecular-mass material, indicates that side-chain interdigitation is unlikely in this modification, just as in form I. Diffraction patterns in which the two crystalline phases coexist show that the longer axis directions in the two forms are approximately orthogonal, suggesting differences in the crystallization process. Very low-molecular-weight systems tend to crystallize preferentially in form II and give rise to a mesophase characterized by very low degrees of order, probably monodimensional. High regioregularity of the samples appears to affect both the intramolecular order and the packing.

Introduction

In the last two decades increasing demand for new polymers has been evidenced in the area of "functional materials" designed for specific applications, often in the electronic and communication technologies. Thiophene-based polymers are the subject of considerable interest due to the chemical versatility of the thiophene ring that leads to macromolecules with various structures and modulated physical and electronic properties. Significant recent progress in the synthesis of thiophene-based polymers has resulted in enhanced processability and stability. The insolubility and the infusibility of polythiophenes have been overcome by the controlled introduction of flexible side groups in the 3-position.[1] The relationship between chemical structure, solid state organization, and physical properties in this family of polymers seems thus highly significant.

The structural characteristics of poly(3-alkylthiophenes) (PAT's) have been intensively studied. X-ray diffraction investigations suggest, for the more common crystalline polymorph of these macromolecules, layered structures where alkyl chains act as spacers between stacks of closely packed planar main chains. The layer thickness in this phase, identified here as form I, was found to vary almost linearly with the length of the aliphatic side chains.[2−5]

A second type of polymorph for the octyl, decyl, and dodecyl derivatives of the poly(3-alkylthiophenes) series has been recently reported.[6−9] This phase is characterized by a substantially shorter "layer thickness" identified by the first strong Bragg diffraction maximum, as compared to form I. Structural models for the second polymorph, which we will call form II, are still less clearly defined. In the literature[6,8] there are, however, suggestions that this phase may present significant interdigitation of the alkyl side chains, as opposed to what is now generally accepted for form I.

In this paper, we report a thermal and structural characterization of various poly(3-decylthiophenes) differing in regioregularity and molecular weight. Besides the two mentioned crystalline modifications, PDT may also adopt a mesomorphic form.[6] The nature and stability of these phases in analogy to those suggested for other polyalkylthiophenes (PAT's) will be discussed together with some pertinent morphological features. We will also see that the accessibility of the different polymorphs and specifically of the mesophase appears to be influenced by molecular weight and by the regioregularity in a qualitatively predictable way.

Experimental Section

Using the synthetic route giving absolute regiocontrol at each coupling step in the polymerization reaction,[10] two regioregular poly(3-decylthiophenes) have been prepared (R-PDT3 and R-PDT14) starting from 2-iodo-3-decylthiophene (yield 78%). By NMR analysis the polymers show more than 99% head-to-tail (HT) couplings.

We have also synthesized the same polymer via oxidative reaction with $FeCl_3$ obtaining a lower head-to-tail regularity.[11,12] The polymer was extracted first in a Soxlet apparatus with diethyl ether, separating a low-molecular-weight fraction (PDT13), and then with chloroform, thus obtaining a higher M_w fraction (PDT180). The head-to-tail regioregularity for both samples was found to be around 70% by NMR spectroscopy. The average molecular weight, M_w, and polydispersity, M_w/M_n for all samples (see Table 1) were determined by GPC (Waters 600E) referred to polystyrene standards in THF.

Differential scanning calorimetry was performed using a Perkin-Elmer DSC-7 system, equipped with a CCA7 liquid nitrogen cooling device. Heating and cooling rates were typically 20 °C/min.

X-ray diffraction patterns were recorded from samples mounted in a glass capillary with a Debye photographic camera using Ni-filtered Cu Kα radiation. A Siemens P4 diffractometer, with graphite monochromated Cu Kα radiation,

[⊗] Abstract published in *Advance ACS Abstracts,* November 15, 1997.

S0024-9297(97)00655-4 CCC: $14.00

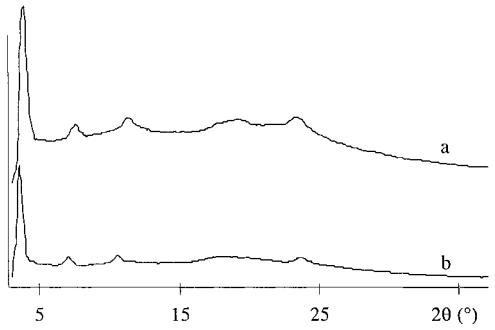

Figure 1. X-ray diffraction patterns of R-PDT14 solution-crystallized samples: trace a is recorded at room temperature while trace b is recorded at 80 °C.

Table 1. Molecular Weights and Polydispersities of Poly(3-decylthiophene) Samples Used in This Investigation

sample	M_w	M_w/M_n
R-PDT3	3 400	1.2
R-PDT14	14 100	1.64
PDT13	13 500	1.93
PDT180	178 000	3.64

equipped with a bidimensional Hi-Star detector and with N_2 thermostated flow (temperature range between −60 and 95 °C), was also used.

Samples for electron microscopy and diffraction were obtained by dissolution in mesitylene. After casting from a dilute mesitylene solution, thin films were melted at 200 °C and then cooled at 0.2 °C/min to room temperature. The films were subsequently shadowed obliquely with Pt/C, coated with amorphous carbon, and floated off their substrates for transmission electron microscopic examination at 100 kV. To minimize radiation damage, electron-diffraction patterns were recorded under low-dose conditions.

Results and Discussion

Regioregular Polymers: R-PDT14 and R-PDT3. Figure 1 shows X-ray diagrams of R-PDT14 crystallized from $CHCl_3$ recorded at room temperature (trace a) and at 80 °C (trace b). In the native sample a strong reflection around $2\theta = 3.8°$ ($d = 22.7$ Å) is apparent with its higher orders at $2\theta = 7.8°$ and 11.6°, respectively. The main peak is generally assigned to the interlayer vector, and in different polyalkylthiophenes this spacing is linearly related to the side-chain length. We will refer to the crystalline phase characterized by this diffraction maximum as form I. A weak reflection at $2\theta = 5.2°$ ($d = 17.0$ Å) and its corresponding very weak higher orders at $2\theta = 10.4°$ and $2\theta = 15.5°$ are much more apparent in photographic patterns than in Figure 1 (see Tables 2 and 3). As we will see, these maxima result from small amounts of a second polymorph (form II). At wider angles in the 18−30° 2θ region there is another series of reflections, with the more prominent peak at $2\theta = 23.2°$ ($d = 3.83$ Å). Although this spacing occurs in a number of polyalkylthiophenes with different side chains and different regioregularity, its value seems slightly too low to relate to the axial periodicity of the polythiophene chain. Consistent with the suggestions of other authors[2,4,5,13] and also with the behavior of this spacing with temperature, it is attributed to intralayer stacking between thiophenic main chains.

X-ray spectra recorded at 80 °C still display a strong and sharp reflection at $2\theta = 3.6°$ together with its higher orders, thus showing a shift to lower angles because of thermal expansion of the layered structure. On the contrary the peak at $2\theta = 23.5°$ ($d = 3.79$ Å) shows a contraction of the interplanar spacing, as already reported for other PAT polymers.[3,4] This behavior, as already noted by Tashiro et al.,[3] is incompatible with a predominantly intrachain origin of the 3.8 Å diffraction maximum and also suggests reorganization rather than simple thermal expansion of the lattice. The other peaks observed at low temperature, such as the weak

Table 2. X-ray Diffraction Data of Native R-PDT14 Crystallized in Form I[a]

2θ (deg)	d_{obs} (Å)	hkl[b]	d_{calc}[b] (Å)	hkl[c]	d_{calc}[c] (Å)	hkl[d]	d_{calc}[d] (Å)
3.8	23.2	100	22.94	100	23.0	100	22.94
7.7	11.5	200	11.48	200	11.5	200	11.5
11.55	7.66	300	7.65	300	7.67	300	7.65
15.5	5.72	400	5.74	400	5.75	400	5.74
						−301	5.61
17.8	5.00	211	4.93	011	4.86	−211	5.00
						211	4.86
19.4	4.58	500	4.59	500	4.60	500	4.59
		410	4.60	−211	4.48	410	4.60
		401	4.61	211		401	4.61
21.7	4.09	(411)	(3.55)	−311	4.10	−501	4.06
				311		−411	4.03
22.9	3.88	002	3.88	002	3.88	002	3.88
23.2	3.83	020	3.83	010	3.83	020	3.83
		600	600	600	600	600	
		102	102			120	3.80
24.9	3.57	220	3.64	−212	3.59	202	3.61
				212		−511	3.58
26.7	3.34	212	3.31	−511	3.34	−212	3.36
				511		−221	3.32
29.4	3.04	412	3.00	−102	3.03	−502	3.05
				102			

[a] Indexing is given assuming analogies with two types of previously suggested PAT lattices. A third indexing, giving a better fit to our data, is also proposed. [b] Orthorhombic cell closely related to those proposed in refs 4 and 13. Lattice parameters: $a = 22.96$ Å; $b = 7.67$ Å; $c = 7.76$ Å; $\rho_{calc} = 1.08$ ($Z = 4$). [c] Monoclinic cell related to the one proposed in ref 5 for POT. Lattice parameters: $a = 23.0$ Å; $b = 4.86$ Å; $c = 7.76$ Å; $\alpha = 52°$; $\rho_{calc} = 1.08$ ($Z = 2$). [d] Monoclinic cell similar to the orthorhombic model but slightly perturbed to better fit our data. Cell parameters: $a = 23.0$ Å; $b = 7.68$ Å; $c = 7.76$ Å; $\gamma = 93.2°$; $\rho_{calc} = 1.08$ ($Z = 4$).

Table 3. X-ray Diffraction Data Relative to Form II Obtained from Solution -Crystallized R-PDT3 (Form I Peaks Have Been Omitted for Clarity)[a]

2θ (deg)	d_{obs} (Å)	hkl[b]	d_{calc}[b] (Å)	hkl[c]	d_{calc}[c] (Å)
5.2	17.0	100	17.02	100	16.92
10.4	8.5	200	8.51	200	8.46
15.6	5.7	300	5.68	300	5.64
		−201	5.73		
		201			
18.0	4.93	−311	4.97	110	4.74
19.5	4.55	020	4.56	−301	4.57
		−301	4.58	301	
		301			
21.5	4.13	−321	4.17	−111	4.18
		−411	4.14		
23.0	3.87	002	3.88	002	3.88
24.5	3.63	−112	3.64	310	3.61
26.4	3.38	−521	3.39	500	3.39
		220	3.38		
28.3	3.16	−231	3.16	302	3.20
				410	3.12

[a] Indexing is given assuming analogies with a lattice type previously suggested for other PAT's. A second lattice, with a better fit to our data and to models discussed in the text, is also proposed. [b] Lattice parameters related to those proposed by Winokur et al.[8] for other PAT's: $a = 19.6$ Å; $b = 10.5$ Å; $c = 7.76$ Å; $\gamma = 119.3°$; $\rho_{calc} = 1.06$ ($Z = 4$). Note that the c axis value was set at 7.76 Å instead of 8.0 Å. [c] Monoclinic cell with c unique axis. Cell parameters: $a = 17.0$ Å; $b = 5.08$ Å; $c = 7.76$ Å; $\gamma = 95.0°$; $\rho_{calc} = 1.10$ ($Z = 2$).

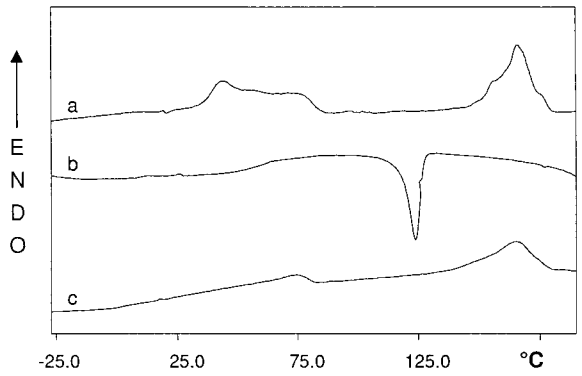

Figure 2. DSC thermograms of R-PDT14 samples recorded at 20 °C/min: trace a is the first heating run of a native sample, trace b is the successive cooling run and trace c is the second heating run.

maximum at $2\theta = 5.2°$ attributed to form II, are not at all discernible at 80 °C. The features of the 80 °C pattern appear compatible with a 2D layered thermotropic mesophase (a = 24.5 Å, b = 3.8 Å), and the narrowing of the peak half-widths is consistent with larger coherent domains expected in a mesomorphic form. Similar suggestions were put forward in previous studies for other PAT's.[3,4,8,9]

On cooling the mesophase or the melt to room temperature, the diffraction profile rather rapidly recovers the features observed with the pristine sample. This fact and the similarities between the diffraction patterns of the mesophase and of form I suggest that between these two phases close analogies must exist: indeed in some samples there is the suspicion that no clear-cut transition is necessarily observed.

DSC data are very helpful in this context. First heating runs on native samples (Figure 2a) show a complex endotherm between 20 and 90 °C (ΔH = 10 J/g) where two maxima are identifiable (T = 44 and 76 °C) while the isotropization occurs around 166 °C (ΔH = 10 J/g). In the cooling run (Figure 2b) we observe an exotherm at 123 °C (ΔH = 8 J/g) due to the crystallization of the mesophase from the melt. The isotropization and the recrystallization processes substantially differ from the reported behavior of other PDT samples[6] but are consistent with recent data on other regioregular PAT's.[9,14] While a second heating run recorded without delay (Figure 2c) only displays the broad endotherms around 76 °C and at 166 °C, after a day at room temperature, samples crystallized either from the melt or from the mesophase present a thermal behavior closely similar to that of the pristine sample.

Since paraffin side chains packed pseudohexagonally melt typically around 40−50 °C,[15] the first observed endotherm in DSC heating runs is quite probably related to this process. Available X-ray data are insufficient to unequivocally confirm this interpretation, as our unoriented diffraction patterns do not show significant variations across this temperature. Consistent with previous studies and with the diffraction data, the endotherm at 76 °C is assigned to the crystalline to mesomorphic transition (T_m), a process which seems to involve both main-chain packing and side-chain melting. In the mesophase, however, the main-chain conformation and its position in the lattice found in form I must in essence be preserved.

The X-ray patterns of native R-PDT3 samples (M_W = 3100) differ (see Figure 3a and Table 3) from those obtained from R-PDT14. The reflection at $2\theta = 5.2°$ (d = 17.0 Å), together with its higher orders, is substantially stronger in this lower molecular mass polymer, indicating that in this sample a different polymorph (form II) prevails. This phase corresponds in essence to the α-phase previously described for P3DT.[6] It is also clearly related to similar phases recently identified for poly(3-octylthiophene)[8,9] and poly(3-dodecylthiophene)[9] which should be characterized by side-chain interdigitation.[8,9] The reflection at 2θ = 3.9−4.0°, typical of mesomorphic and of form I samples, is also present in diffraction patterns of pristine R-PDT3 but is relatively weak. It becomes predominant only in specimens crystallized from the melt (Figure 3, trace b).

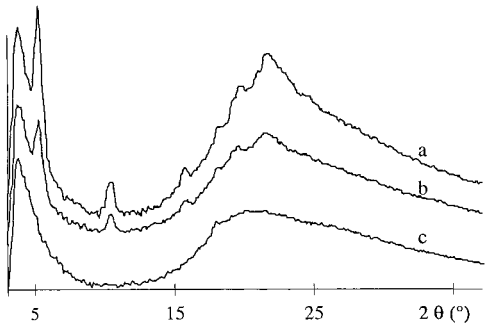

Figure 3. X-ray diffraction patterns of R-PDT3: trace a is recorded on a native sample at room temperature, trace b is taken on a melt-crystallized sample, and trace c is recorded at 70 °C.

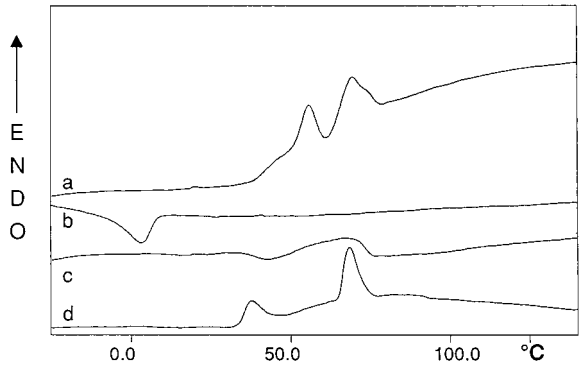

Figure 4. DSC thermograms measured for R-PDT3 samples: trace a is the first heating run, trace b is the cooling run, trace c is the second heating run, and trace d is the heating run on a room-temperature melt-crystallized sample, subsequently annealed at 60 °C (heating and cooling rates 20 °C/min).

The patterns of pristine R-PDT3 recorded at *ca.* 75 °C (see Figure 3c) present only one rather sharp reflection at $2\theta = 3.8°$ and a broad halo in the wide-angle region, consistent with a mesomorphic organization of R-PDT3 very similar to the one previously reported[6] for a less stereoregular, low-molecular-weight sample of PDT. The broad featureless hump centered at $2\theta = ca.$ 20° indicates that locally the sample is in essence amorphous. The substantial differences between the R-PDT3 and the R-PDT14 mesophases are related to their different molecular masses and will be discussed after the thermal characterization of R-PDT3.

The first DSC heating run on a solution-crystallized sample of R-PDT3 (Figure 4a) shows only two poorly resolved endothermic peaks centered respectively at 54 °C (ΔH = 5.5 J/g) and 68 °C (ΔH = 7.5 J/g). On cooling, an exothermic transition occurs at 4 °C (ΔH = 6 J/g) while the successive heating (Figure 4c) shows again two broad endotherms but of lower intensity: a first one around 33 °C (ΔH = 0.5 J/g) and a second one in the same temperature range as observed in the first run.

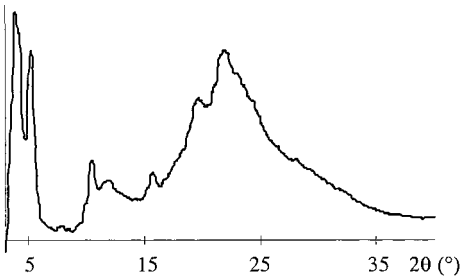

Figure 5. X-ray diffraction patterns recorded at 25 °C of R-PDT14 recrystallized from a $CHCl_3/CH_3OH$ solution.

DSC scans of melt-crystallized samples, subsequently annealed at 60 °C for 1 h (Figure 4d), still present two endotherms which, however, are clearly resolved while presenting enthalpy values comparable to those from pristine samples: the first transition occurs around 38 °C ($\Delta H = 4$ J/g) while the second occurs again at 68 °C ($\Delta H = 7.4$ J/g). This behavior critically confirms previous findings[6] and, consistent with X-ray patterns (not shown) which indicate a prevalence of form II, suggests that annealed samples are very similar to the native solution-crystallized specimen. It implies also that form II is likely to be under ambient conditions the thermodynamically stable crystal phase.

While the lower temperature transition is related to the disordering of the side chains, as already suggested for R-PDT14, the endotherm at 68 °C is probably due to the transition from the crystalline phase to the mesomorphic phase. The isotropization process is thus not apparent in the thermograms, but optical investigations suggest a T_i around 100 °C. The transition may be too broad and its enthalpy too small to be evidenced by DSC because of the specific features of the R-PDT3 mesophase. Considering both the undercooling and the associated enthalpy, the transition observed on cooling at 4 °C (Figure 4b) should not be due to the crystallization of the mesophase but of form II directly from the isotropic state or from the mesophase.

Summarizing, we can state that whereas form I is accessible to both R-PDT14 and R-PDT3, although more readily for the former sample, phase II crystallizes much more efficiently with the low-molecular-weight system and in fact we are not aware of any thermal treatment giving significant proportions of form II with R-PDT14. This could be achieved only by crystallization from solution, consistent with the results of previous studies.[6−9] We used a solvent−nonsolvent mixture ($CHCl_3$ and CH_3OH), and the recrystallized samples present X-ray patterns (see Figure 5) where the intensity of the form II reflection at $2\theta = 5.2°$ is comparable to that of the form I reflection at $2\theta = 3.8°$.

DSC thermograms of these samples (Figure 6) show only a comparatively sharp endotherm around 80 °C ($\Delta H = 18$ J/g), due to the crystalline−mesophase transition, aside from the R-PDT14 isotropization endotherm (T_i) at the usual temperature of 166 °C (see Figure 2, trace a). The low-temperature (30−50 °C) transition, associated with side-chain disordering, seems to be missing in these samples, or it appears rather to coalesce with the crystalline−mesophase transition. These processes can either proceed independently or coincide (probably as a function of crystal perfection), while the specific crystalline modification (form I or form II) hardly seems to matter either in this respect or, as far as we could determine, for the crystalline−mesophase transition temperature.

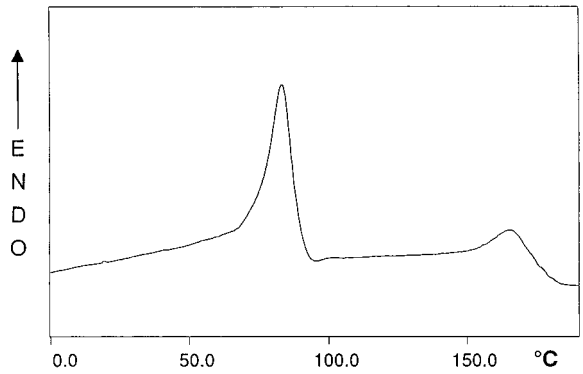

Figure 6. First DSC heating run of a R-PDT14 sample recrystallized from a $CHCl_3/CH_3OH$ solution.

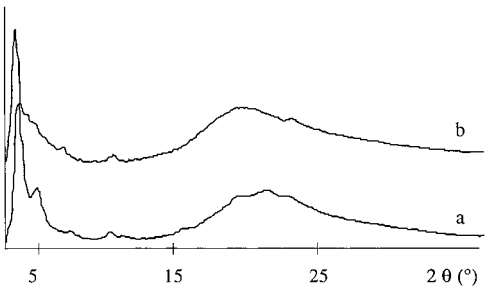

Figure 7. X-ray diffraction patterns of PDT13 samples: traces a and b are recorded on a native sample at room temperature and at 80 °C, respectively.

The second striking difference between the two regioregular samples of different molecular mass concerns the mesomorphic behavior. The thermal analysis evidences that the mesophase of the higher molecular mass sample should be thermodynamically stable between *ca.* 80 and 160 °C while for R-PDT3 the mesomorphic range contracts substantially. For this sample the mesomorphic phase may possibly have only kinetic stability. Also the order evidenced by diffraction data for the two mesophases differs substantially: in the case of R-PDT14, bidimensional (2D) projection order is preserved and domains must be large, as evidenced in the relative sharpness of the diffraction maxima (see Figure 1b). For the lower molecular mass polymer, mesomorphic order may reduce to a one-dimensional layer-like structure, since the stacking reflection at $d = 3.8$ Å is not observed; in any case for R-PDT3 either two- or one-dimensional order will be only relatively short-range because of the broadness of the observed reflections (see Figure 3c).

Defective Polymers: PDT13 and PDT180. We have studied the PDT13 and PDT180 samples to explore how the presence of chain defects can affect the existence of the crystalline modifications (phase I and phase II) and of the mesophase. Native PDT13 with a molecular weight very close to that of R-PDT14 but a lower (70% as opposed to 99%) HT regioregularity yields X-ray patterns (Figure 7a) very similar to that of R-PDT14. In native PDT13 phases I and II coexist, but the proportion of phase II is clearly higher than that in R-PDT14. This is evidenced in the greater relative intensity of the reflection at $2\theta = 5.2°$. Furthermore in the less regioregular polymer, reflections are somewhat broader and the patterns display lower crystallinity while *d*-spacings are slightly expanded, as would be expected for a defective system. At temperatures above 70 °C, phase II peaks disappear and diffraction patterns of PDT13 (Figure 7b), like those obtained in similar conditions with R-PDT14 (Figure 1b), suggest a 2D mesophase. However, peaks are broader and domains

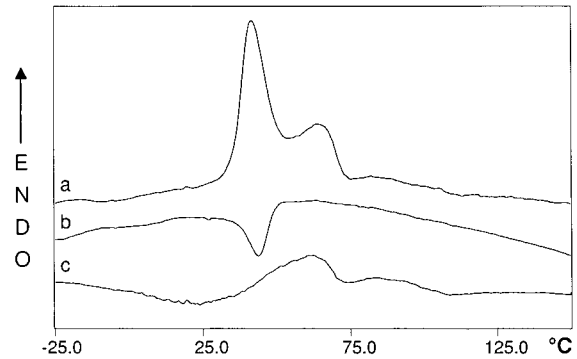

Figure 8. PDT13 thermograms recorded at 20 °C/min: trace a is the first heating run, trace b is the subsequent cooling run, and trace c is a heating run after crystallization from the melt.

accordingly smaller. There are clear indications of a high amorphous content, as in the mesophase of the lower molecular mass R-PDT3 (Figure 3c).

DSC runs (Figure 8) show that the thermal behavior of PDT13 is more similar to that of the low-molecular-weight R-PDT3 than to that of R-PDT14, and the assignment of the transitions is straightforward after the discussion of the regioregular samples. In the first heating run the two usual low-temperature endotherms at 43 °C (ΔH = 10 J/g) and at 66 °C (ΔH = 4.7 J/g) are well defined; there are only weak indications of a very broad isotropization transition between 80 and 110 °C, which are further confirmed by optical microscopy. Crystallization occurs on cooling at 43 °C (ΔH = 3 J/g) and is probably a transition from the melt to the 2D-phase. In the second heating only a broad asymmetric endotherm centered at 61 °C (ΔH = 14 J/g) is detected other than the above-mentioned broader process between 80 and 110 °C. After 1 day at room temperature the DSC and X-ray patterns (not shown) become similar to the ones presented by the pristine sample.

The clearest difference between the two systems of comparable molecular weight but different regio-order (R-PDT14 and PDT13) is the temperature stability of the mesomorphic phase, which is greatly reduced for PDT13 and is in fact rather similar to that of R-PDTR3. The nature of the 2D-mesophase and the tendency to crystallize into form I are shared by the two samples of similar molecular weight. However, the regiodefects appear to act in the same direction as a reduction in molecular weight by introducing a bias favoring form II; they also lead to a smaller domain size and a lesser degree of order in the mesophase. All these features are also characteristic of the low-molecular-mass R-PDT3 sample.

With the high-molecular-weight PDT180 sample (M_w = 180 000) the existence window of the mesophase is again quite broad: in typical DSC scans (not shown) the crystalline−mesophase transition occurs as expected between 65 and 70 °C while a clear isotropization process is observed around 140 °C. The exotherm observed on cooling is centered around 70 °C and must therefore be related to the transition from the melt to the 2D-phase, as found in the other samples (R-PDT14 and PDT13) of relatively high molecular weight. X-ray diagrams (not shown) indicate that the only crystalline phase present in this system is form I.

Morphological Observations and Structural Discussion. Electron microscopic observations were limited to the regioregular samples because of the inherently poor tendency toward crystallization of poly(3-decylthiophene). The available quantity of R-PDT3 was insufficient, and thus we had to limit our investigation to the higher molecular mass R-PDT14. Melt crystallized thin films generally display uniform morphologies that reveal no distinct crystallites even at very high magnifications (see Figure 9). Occasionally bloblike features 200−300 nm in diameter are seen. The corresponding electron diffraction patterns (Figure 10) reveal that the samples are polycrystalline and unoriented on the plane of the film. Surprisingly but consistent with recent reports on other PAT's,[16] only the 3.8 Å reflection, attributed to the stacking distance in form I or in the mesophase, is apparent. There is no evidence of the very strong 23 Å maximum associated with layer thickness nor of its higher orders, even upon tilting the sample stage up to 60°. These facts indicate that layers must be close to parallel to the substrate surface (since in electron diffraction only the crystallographic planes that are oriented parallel to the electron beam yield observable reflections). Indeed also X-ray diffraction patterns of melt- or solution-crystallized R-PDT14 (Figure 11) show that a^* in form I samples is preferentially oriented perpendicular to the film surface.

In a few specimen regions for R-PDT14, very small and immature spherulites could be identified by electron microscopy. The corresponding diffraction patterns

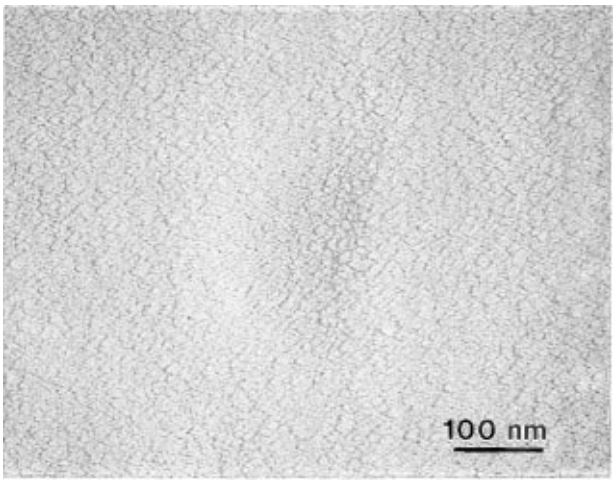

Figure 9. Transmission electron micrograph obtained from R-PDT14 crystallized by cooling from 200 °C to room temperature at 0.2 °C/min.

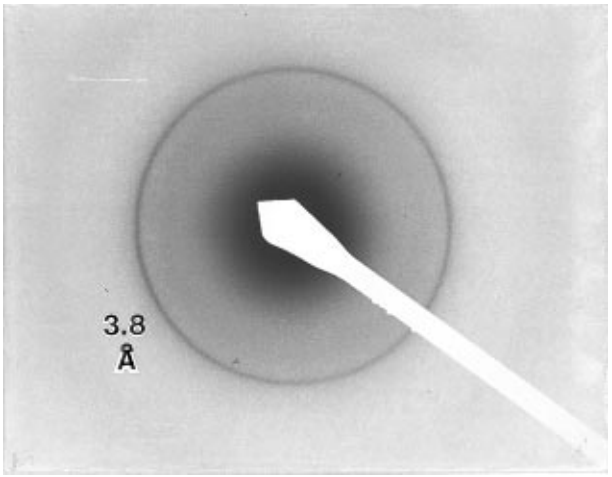

Figure 10. Electron diffraction pattern obtained from R-PDT14 crystallized by cooling from 200 °C to room temperature at 0.2 °C/min.

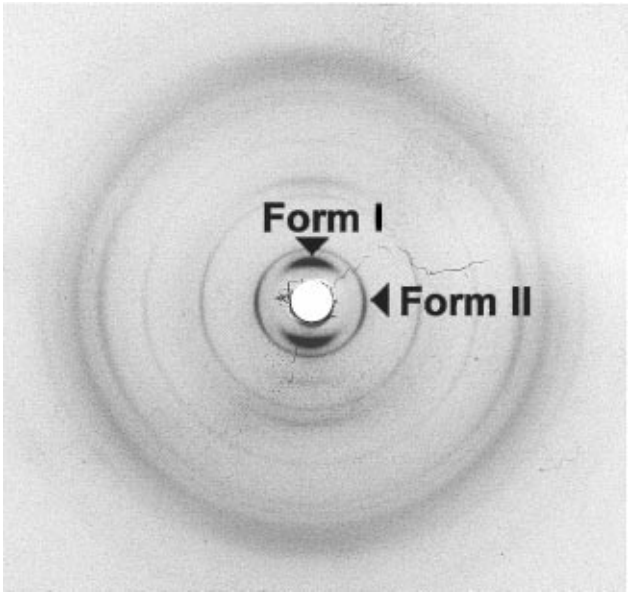

Figure 11. X-ray diffraction pattern showing coexistence of the two crystalline polymorphs of PDT with different modes of orientation. The pattern was obtained from a sample of R-PDT14 crystallized from a $CHCl_3/CH_3OH$ solution and was recorded edge-on. The normal to the PDT film is vertical in the figure.

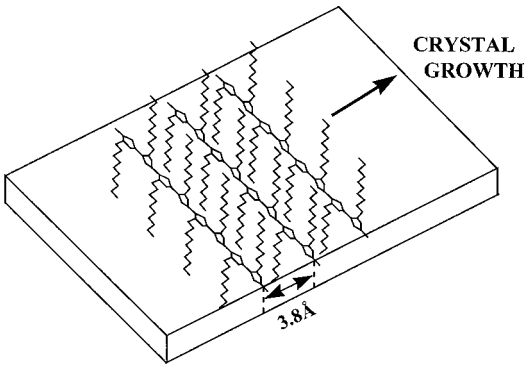

Figure 12. Schematic of the crystal growth mechanism in form I.

from these very small structures were far too weak to be captured on photographic film. However, when observed on the fluorescent screen, they consistently indicated that the radial direction, *i.e.* the preferred growth direction, corresponds to the 3.8 Å stacking among main chains. This evidence appears consistent with the fact that the alkyl side chains dictate form I nucleation on the substrate, giving rise to the characteristic lamellar structure, a morphology preserved also in mesomorphic samples. This layered structure in turn allows the main chains to approach to a distance of 3.7−3.8 Å, giving rise to a stacking which develops with comparative ease (see schematic of Figure 12). Additional order in the third dimension develops if at all with great difficulty in form I and mesomorphic structures.

No electron microscopic evidence on form II is available at present. However, X-ray diffraction patterns (Figure 11) of solution-crystallized R-PDT14 show that for this crystalline modification the longer lattice spacing is preferentially oriented in the plane of the film; *i.e.*, it is orthogonal to the corresponding form I direction. This points to a nucleation mechanism that is different in the two polymorphs. A more detailed interpretation requires reliable models for the crystalline structures of both modifications.

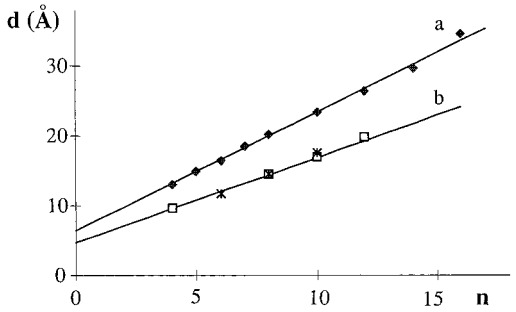

Figure 13. Largest observed interplanar distances *d*, corresponding to the lattice vector *a*, for form I (trace a) and form II (trace b), versus the number of carbon atoms in the side chain *n*. Points $n = 4-8$, 12, 14, and 16 are taken from refs 3−9, 13, 14, and 17−21.

Using our findings on poly(3-decylthiophenes), literature data[3−9,14,17−20] on other poly(3-alkylthiophenes), and preliminary results on poly(3-butylthiophenes),[21] we have plotted (Figure 13) the interplanar distances *d* corresponding to the first diffraction maxima belonging respectively to phase I and phase II versus the number of carbon atoms in the alkyl side chains. For both polymorphs the above-mentioned spacing increases with the number of side-chain carbons *n* in an essentially linear relationship. Deviations from a linear dependence for form I were interpreted by Gustaffson et al.[2] as an indication of partial side-chain interdigitation but may result from uncertainties associated with measurements. Alternatively, longer side chains may adopt increasingly disordered and thus more contracted conformations. The data summarized in trace *a* of Figure 13 are consistent with the form I structure proposed by Winokur et al.,[4] which is characterized by side chains showing a modest tilt (*ca.* 30°) with respect to the plane of the main chain (see Figure 14a). In such models the long axis of the unit cell is also nearly coplanar with the main chain and side-chain interdigitation does not occur. Interdigitation appears to us generally entropically disfavored and, in the case of form I, unlikely considering the close relationship that exists between this polymorph and the 2D mesomorphic phase. Trace *b* of Figure 13 evidences that the above arguments regarding the likelihood of interdigitation apply also to form II data.

It is quite interesting to note that available diffraction data pertaining to HH−TT regioregular poly(3,3′-dialkyl-2,2′-bithiophenes), in the cases of hexyl,[22] octyl,[22,23] and decyl[22] substituents, also fit remarkably well the line determined for form II regioregular HT poly(3-alkylthiophenes) (× marks on trace b of Figure 13). This surprising coincidence between the longer interchain *d* spacing of phase II HT polymers and the crystalline phase of HH−TT polymers could be interpreted in terms of identical degrees of interdigitation in the structures of the two families of polyalkylthiophenes. This appears however once again unlikely, and this behavior is a strong additional indication of non-interdigitating side chains also in the case of form II structures, for which regioregularity appears to have hardly any influence.

The main-chain periodicity for all PAT's must be a multiple of 3.88 Å, and for each member of the poly(3-alkylthiophene) series closely comparable densities of the two crystalline modifications are expected. Under these assumptions first approximation, one-chain unit cell or subcell models of modification II for all the PAT's referred to in Figure 13 may be devised involving non-interdigitated layered structures with an intralayer stacking close to 5.2 Å (Figure 14b).

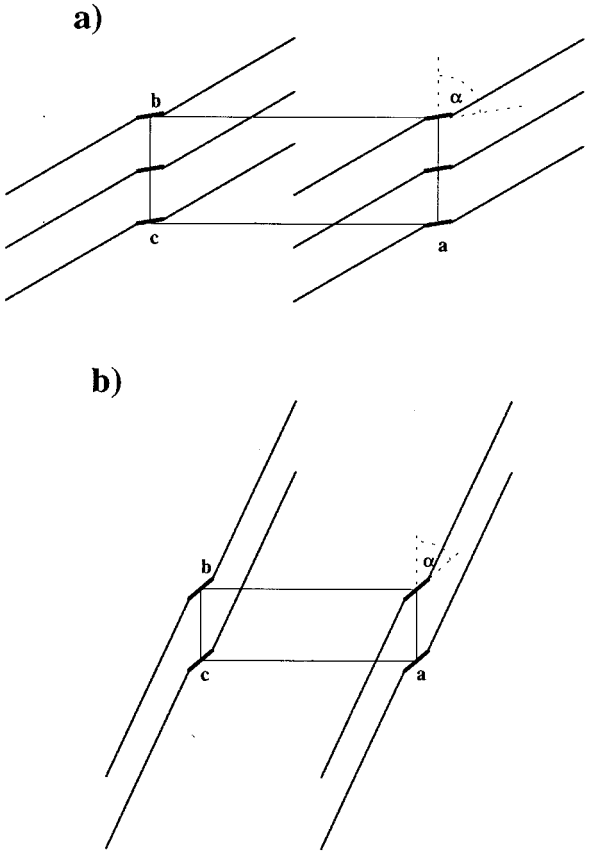

Figure 14. Schematic models of the packing of crystalline poly(3-decylthiophene) in (a) form I adapted from ref 8 and (b) form II.

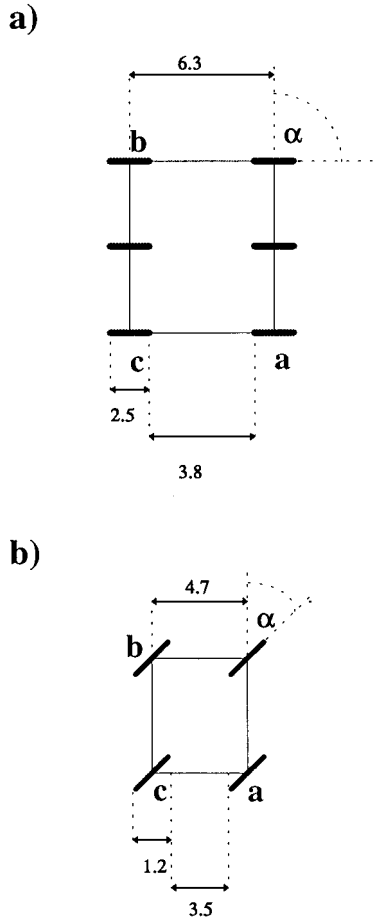

Figure 15. Hypothetical form I (a) and form II (b) PAT lattice models extrapolated to unsubstituted polythiophene (dimensions in angstroms). The 6.3 and 4.7 Å values for the *a*-axis are the intercepts of the least-squares lines for the form I and II PAT structures in Figure 13.

The 3.8 Å intralayer stacking proposed for all form I PAT structures implies that in this phase the planar main chains are arranged in graphite-like stacks close to perpendicular to the *b* axis, *i.e.* with a setting angle α of *ca.* 90° (Figure 14a). The value of 6.3 Å for the *a* axis of a hypothetical unsubstituted polythiophene form I, estimated by extrapolation from the poly(3-alkylthiophene) data (*i.e.* for $n = 0$, trace a in Figure 13), corresponds indeed well with the lateral steric requirements of a layer of polythiophene chains with the setting angle α equal to 90°.

The *a* axis of a hypothetical unsubstituted form II (obtained as for form I, in this case by extrapolation from the data in Figure 13, trace b) is 4.7 Å and suggests that the setting angle α for this polymorph (see Figures 14b and 15b) is substantially lower than 90°. It is noteworthy that the *ca.* 5.2 Å *b* axis value suggested for form II PAT's is shorter but comparable to the *b* axis value (5.72 Å) in the polythiophene crystal structure,[24] where this axis also corresponds to a stacking periodicity and the setting angle α measures 30°.

A final comment concerns the fact that the UV data indicate that the increase in conjugation length with regioregularity is more marked in the solid state than in solution. Such an effect should be related to intermolecular effects (*i.e.* better packing).[25] Our room-temperature diffraction data for form I show that regioregularity and crystallization conditions affect primarily the periodicity along *a* while the interchain stacking *b* retains a value of 3.80 ± 0.02 Å that is hardly sensitive to any of these factors. The relatively disordered side-chain packing found *e.g.* in the mesophase may lead to somewhat closer packing along the *b* direction (*vide supra*). On the contrary the interstack spacing *a* is 24.0 Å for the regioirregular PDT180 but only 23.7 Å and 22.7 Å, respectively, for melt- and solution-crystallized regioregular R-PDT14, pointing to better side-chain packing as a key issue. Thus the increased conjugation length and the better main-chain packing, both resulting because of conformational properties of the regioregular PAT chain, are certainly related to each other but in a way that requires further data to be fully understood. A complete structural refinement of form II structures would indeed be very helpful.

Concluding Remarks

The above discussion demonstrates that for poly(3-decylthiophenes) crystallization of the two different polymorphs depends more on molecular weight than on chain defects. Since similar phases are observed for poly(3-alkythiophenes) with different alkyl side chains, our findings probably also apply to such other systems. With high-molecular-weight samples like PDT180 we found that, consistent with the data in the literature, form I is obtained exclusively and form II contributions are normally negligible. While with the less regioregular PDT13 sample of moderate molecular mass (13 000) some form II readily develops also from the melt, with the regioregular R-PDT14 sample of closely similar molecular mass it is possible to obtain phase II only by recrystallization from solution. We can simply conclude that both lower molecular mass and regioregularity defects favor form II over form I, and this seems

reasonable, since chain ends can be considered as a kind of defect. Similar observations have recently been discussed in the case of the polymorphic behavior of polypropylene[26] and may relate to the side-chain tilt relative to the crystal surface or to bulk effects.

Heating phase I yields generally a 2D-mesophase which shows substantial thermodynamic stability. Upon cooling, this reasonably well organized mesophase reverts readily to phase I with concomitant or subsequent side-chain crystallization. Both regioregularity defects and molecular mass influence the existence window of this mesophase: less regioregular PDT13 samples of similar molecular mass present an isotropization temperature T_i more than 50 °C lower than that of regioregular R-PDT14 samples. This difference is reduced to 30 °C with high-molecular-mass PDT180. For very low-molecular-weight polymers such as R-PDT3, the existence domain of the mesophase is also greatly reduced in spite of the regioregularity and there is a possibility that the mesophase is only kinetically stable (*i.e.* it is metastable). Apparently the R-PDT3 mesophase has only a one-dimensional or lamellar order and is characterized by substantially smaller domain dimensions, as gauged from the diffraction peak width. Indeed, it seems that, for this very low molecular-mass material (M_w = 3000), the degree of order in the mesophase is only marginally higher than that in the amorphous phase. Upon cooling this mesophase, crystallization of phase II rather than of phase I occurs, and it is still somewhat unclear whether this is due to thermodynamic or kinetic reasons. However, the annealing behavior of R-PDT3 suggests that form II is the stable phase and that therefore form I is favored essentially by kinetic factors in high-molecular-mass samples.

The difficulty to obtain pure form II may account for the fact that the models available for this phase in the literature[6,8] are still contradictory. Our suggestion is based on a structural correlation that seems to work well for form I and must be considered a first-order approximation. The main features of form II appear to be (i) noninterdigitating side chains and (ii) stacking of polyalkylthiophene chains with a periodicity close to 5.2 Å and values of the setting angle α substantially smaller than those in form I. In any case the bulk or film properties of high-molecular-weight PAT's should clearly depend primarily on structural organization in form I or in the mesomorphic phase which predominates in such samples.

The effect of molecular weight and regioregularity on the existence window of the PDT mesophase can be rationalized in terms of free energy versus temperature diagrams, as proposed by Percec and Keller.[27] In essence defects and chain ends should hardly alter the entropic contribution to the free energy in the crystal or in mesomorphic samples but will increase the entropy of the melt, reducing the upper limit of the stability range of the mesophase.

References and Notes

(1) Jen, K. Y.; Miller, G. C.; Elsenbaumer, R. L. *J. Chem. Soc., Chem. Commun.* **1986**, 1346.
(2) Gustafsson, G.; Inganäs, O.; Österholm, H.; Laakso, J. *Polymer* **1991**, *32*, 1574.
(3) Tashiro, K.; Ono, K.; Minagawa, Y.; Kobayashi, M.; Kawai, T.; Yoshino, K. *J. Polym. Sci., Part B: Polym. Phys.* **1991**, *29*, 1223.
(4) Prosa, T. J.; Winokur, M. J.; Moulton, J.; Smith, P.; Heeger, A. J. *Macromolecules* **1992**, *25*, 4364.
(5) Mardälen, J.; Samuelsen, E. J.; Gautun, O. R.; Carlsen, P. H. *Synth. Met.* **1992**, *48*, 363.
(6) Bolognesi, A.; Porzio, W.; Provasoli, F.; Ezquerra, T. *Makromol. Chem.* **1993**, *194*, 817.
(7) Bolognesi, A.; Catellani, M.; Destri, S.; Porzio, W. *Makromol. Chem. Rapid Commun.* **1991**, *12*, 9.
(8) Prosa, T. J.; Winokur, M. J.; McCullough, R. D. *Macromolecules* **1996**, *29*, 3654.
(9) Bolognesi, A.; Porzio, W.; Zhuo, G.; Ezquerra, T. *Eur. Polym. J.* **1996**, *32*, 1097.
(10) McCullough, R. D.; Lowe, R. D.; Jayaraman, M.; Anderson, D. L. J. *J. Org. Chem.* **1993**, *58*, 904.
(11) Yoshino, K.; Nakajima, S.; Onoda, M.; Sugimoto, R. *Synth. Met.* **1989**, *28*, C349.
(12) Österholm, J. E.; Laakso, J.; Nyholm, P.; Isotalo, H.; Stubb, H.; Inganäs, O.; Salaneck, W. R. *Synth. Met.* **1989**, *28*, C435.
(13) Tashiro, K.; Kobayashi, M.; Morita, S.; Kawai, T.; Yoshino, K. *Synth. Met.* **1995**, *69*, 397.
(14) Yang, C.; Orfino, F. P.; Holdcroft, S. *Macromolecules* **1996**, *29*, 6510.
(15) Platé, N. A.; Shibaev, V. P. *Comb-Shaped Polymers and Liquid Crystals*; Plenum Press: New York and London, 1987.
(16) Bao, Z.; Dodabalapur, A.; Lovinger, A. J. *Appl. Phys. Lett.* **1996**, *69*, 4108.
(17) Ekeblad, P. O.; Inganäs, O. *Polym. Commun.* **1991**, *32*, 436.
(18) Bolognesi, A.; Catellani, M.; Destri, S.; Maschерpa, M.; Musco, A.; Porzio, W. In *Materials for photonic devices*; D'Andrea, A., et al., Eds.; World Scientific: London, 1991; p 302.
(19) Porzio, W.; Bolognesi, A.; Destri, S.; Catellani, M.; Bajo, G. *Synth. Met.* **1991**, *41*, 537.
(20) Chen, T. A.; Wu, X.; Rieke, R. D. *J. Am. Chem. Soc.* **1995**, *117*, 233.
(21) Meille, S. V.; Romita, V.; Catellani, M. To be published.
(22) Luzny, W.; Rokita, P.; Zareba, R.; Kulszewicz-Bajer, I. *Synth. Met.* **1995**, *75*, 49.
(23) Märdalen, J.; Fell, H. J.; Samuelsen, E. J.; Bakken, E.; Carlsen, P. H. J.; Andersson, M. R. *Macromol. Chem. Phys.* **1995**, *196*, 553.
(24) Brückner, S.; Porzio, W. *Makromol. Chem.* **1988**, *189*, 961.
(25) Fell, H. J.; Samuelsen, E. J.; Als-Nielsen, J.; Grübel, G.; Märdalen, J. *Solid State Commun.* **1995**, *94*, 843.
(26) Brückner, S.; Phillips, P. J.; Mezghani, K.; Meille, S. V. *Makromol. Rapid Commun.* **1997**, *18*, 1.
(27) Percec, V.; Keller, A. *Macromolecules* **1990**, *23*, 4347.

MA970655T